

SHORT REPORT

The E3 ubiquitin ligase Mib1 regulates Plk4 and centriole biogenesis

Lukas Čajánek*, Timo Glatter and Erich A. Nigg‡

ABSTRACT

Centrioles function as core components of centrosomes and as basal bodies for the formation of cilia and flagella. Thus, effective control of centriole numbers is essential for embryogenesis, tissue homeostasis and genome stability. In mammalian cells, the centriole duplication cycle is governed by Polo-like kinase 4 (Plk4). Here, we identify the E3 ubiquitin ligase Mind bomb (Mib1) as a new interaction partner of Plk4. We show that Mib1 localizes to centriolar satellites but redistributes to centrioles in response to conditions that induce centriole amplification. The E3 ligase activity of Mib1 triggers ubiquitylation of Plk4 on multiple sites, causing the formation of Lys11-, Lys29- and Lys48-ubiquitin linkages. These modifications control the abundance of Plk4 and its ability to interact with centrosomal proteins, thus counteracting centriole amplification induced by excess Plk4. Collectively, these results identify the interaction between Mib1 and Plk4 as a new and important element in the control of centriole homeostasis.

KEY WORDS: Cell cycle, Centriole, Centrosome, Kinase, Ubiquitin, Mib4, Plk4

INTRODUCTION

Centrioles play important functions in the organization of microtubule arrays. A pair of centrioles, surrounded by pericentriolar material (PCM), constitutes the centrosome, the main microtubule-organizing center of animal cells (Bornens, 2012; Gönczy, 2012; Nigg and Stearns, 2011). In addition, centrioles function as basal bodies, or templates, for the axonemes of cilia and flagella (Ishikawa and Marshall, 2011; Santos and Reiter, 2008). In proliferating cells, centrioles duplicate exactly once per cell cycle through the formation of one new centriole close to the proximal end of each pre-existing centriole (Azimzadeh and Bornens, 2007; Firat-Karalar and Stearns, 2014; Nigg and Stearns, 2011). Proper control of centriole biogenesis is crucial for embryogenesis, tissue homeostasis and genome stability (Bettencourt-Dias et al., 2011; Godinho and Pellman, 2014; Chavali et al., 2014; Nigg et al., 2014). Dysfunction of the centriole-ciliary apparatus and/or centrosomes is implicated in the etiology of ciliopathies, brain diseases, dwarfism and cancer (Bettencourt-Dias et al., 2011; Godinho and Pellman, 2014;

Hildebrandt et al., 2011; Nigg and Raff, 2009; Thornton and Woods, 2009).

Centriole biogenesis in human cells and *Drosophila melanogaster* is governed by Polo-like kinase 4 (Plk4, also known as Sak), a distant member of the Polo kinase family (Bettencourt-Dias et al., 2005; Habadanck et al., 2005); in *Caenorhabditis elegans* an analogous function is attributed to the kinase ZYG-1 (O'Connell et al., 2001). Tight control of Plk4 levels is crucial, as its depletion leads to a gradual loss of centrioles and its overexpression to centriole amplification (Bettencourt-Dias et al., 2005; Habadanck et al., 2005; Kleylein-Sohn et al., 2007; Rodrigues-Martins et al., 2007). One important mechanism for controlling Plk4 abundance is based on the ability of Plk4 to dimerize and trans-autophosphorylate, which results in the generation of a phosphodegron for recognition by Skp, Cullin, F-box containing complex coanating β -TrCP ($SCF^{\beta-TrCP}$), an E3 ligase, and subsequent degradation of Plk4 by the proteasome (Cunha-Ferreira et al., 2013; Cunha-Ferreira et al., 2009; Guderian et al., 2010; Holland et al., 2012; Holland et al., 2010; Klebba et al., 2013; Sillibourne et al., 2010). Other regulatory mechanisms are likely to exist, and a full understanding of Plk4 regulation is important, particularly in view of the frequent deregulation of this kinase in human cancers (Chng et al., 2008; Macmillan et al., 2001; Mason et al., 2014; van de Vijver et al., 2002) and the impact of Plk4 mutations on brain development and body growth (Martin et al., 2014).

Here, we report on a new interaction between Plk4 and the E3 ubiquitin ligase Mind bomb 1 (Mib1). This comes as a surprise, as Mib1 has previously been studied mainly in the context of Notch and nuclear factor (NF)- κ B signaling (Barsi et al., 2005; Daskalaki et al., 2011; Itoh et al., 2003; Li et al., 2011; Liu et al., 2012). However, recent reports have described associations of Mib1 with centriolar satellites, small multiprotein clusters in the vicinity of centrosomes (Akimov et al., 2011; Jakobsen et al., 2011; Tollenaere et al., 2014; Villumsen et al., 2013). Here, we confirm that Mib1 localizes to centriolar satellites but additionally show that Mib1 relocates to centrioles in response to stimulation of centriole biogenesis. Moreover, we demonstrate that Mib1 interacts with Plk4 and promotes its ubiquitylation. This in turn affects Plk4 abundance and localization, with important consequences for centriole homeostasis.

RESULTS AND DISCUSSION

Recent proteomics and yeast two-hybrid studies have hinted at a centrosome-associated function for the E3 ubiquitin ligase Mib1 (Akimov et al., 2011; Jakobsen et al., 2011; Tseng et al., 2014). In line with these results, we found that Mib1 colocalizes with PCM-1 (Fig. 1A, top left), a marker for centriolar satellites (Dammermann and Merdes, 2002). Furthermore, we could detect Mib1 in the vicinity of centrosomes in interphase but not mitotic cells (supplementary material Fig. S1), in agreement with

Biozentrum, University of Basel, Klingelbergstrasse 50/70, 4056, Basel, Switzerland.

*Present address: Department of Histology and Embryology, Faculty of Medicine, Masaryk University, Kamenice 3/A1, 62500 Brno, Czech Republic.

‡Author for correspondence (erich.nigg@unibas.ch)

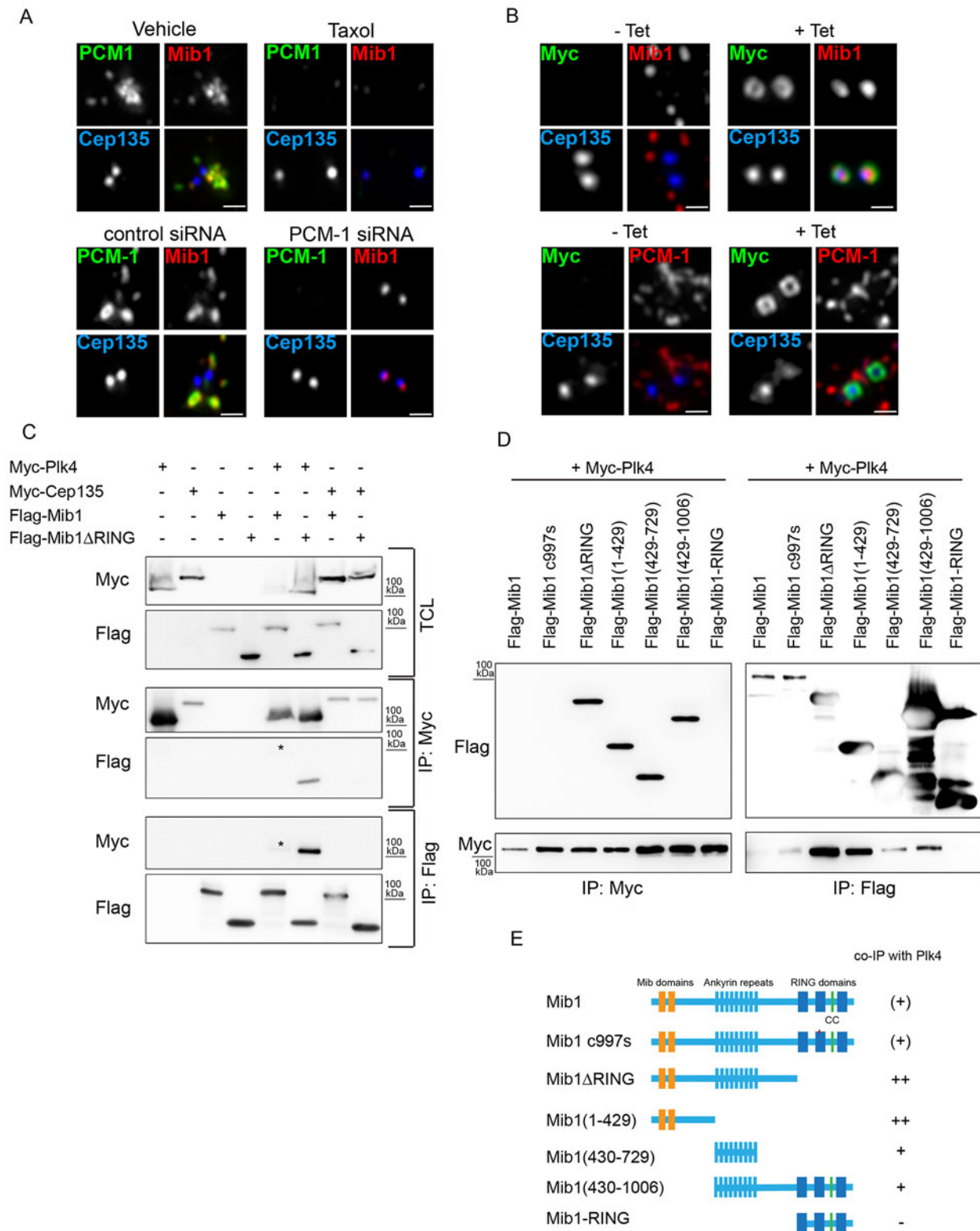


Fig. 1. Interaction of Mib1 with Plk4. U2OS (A) or U2OS:MyC-Plk4 cells (B) were fixed and stained with the indicated antibodies. Scale bar: 0.5 μ m. (A) Cells were synchronized in S phase (aphidicolin, 24 h) and treated for 4 h with vehicle or taxol (5 μ M); siRNA-treated cells were synchronized in S phase and fixed 48 h after transfection, and stained for PCM-1 (green), Mib1 (red) and the centriole marker Cep135 (blue). (B) Control (-Tet) or tetracycline (+Tet)-treated (12 h) U2OS:MyC-Plk4 cells were stained with the indicated antibodies. (C,D) Western blot analyses of immunoprecipitated (IP) complexes from HEK293T cells transfected with the indicated construct. Asterisk denotes detection of a weak band corresponding to the complex between Plk4 and full length Mib1. TCL, total cell lysate. (E) Schematic representation of Mib1 domains interacting with Plk4. Symbols (+), +, ++, or - refer to the efficacy of co-immunoprecipitation.

reports of PCM-1 localization (Balczon et al., 1994). Centriolar satellite localization of both Mib1 and PCM-1 was abolished by taxol treatment, suggesting a dependency on intact microtubules (Fig. 1A, top right). Moreover, siRNA-mediated depletion of PCM-1 resulted in a redistribution of Mib1 to centrioles (Fig. 1A, bottom), reminiscent of the behavior of the centriolar satellite proteins Cep72 and Cep290 (Lopes et al., 2011; Stowe et al., 2012). Furthermore, overexpression of Myc-Plk4 in either U2OS or RPE-1 cells also triggered re-localization of Mib1, but not PCM-1, to centrioles (Fig. 1B; supplementary material Fig. S2A,B). The same phenotype was seen when Plk4 levels were raised through depletion of β -TrCP (supplementary material Fig. S2C) or when centriole amplification was induced through transient transfection of Plk4 or the centriole duplication factors STIL or Sas6 (also known as SASS6) (supplementary material Fig. S2D). Moreover, MCF-7 breast cancer cells, which are prone to centriole over-duplication upon loss of p53 (D'Assoro et al., 2004), showed increased levels of Plk4 and, concomitantly, more pronounced Mib1 signals at centrioles, when compared to RPE-1 cells (supplementary material Fig. S2E–G). Thus, we conclude that Mib1 localizes to centrioles in response to Plk4 elevation and centriole over-duplication, raising the prospect of a functional link between Mib1 activity and the regulation of centriole duplication.

Next, we examined a possible interaction between Mib1 and Plk4. Only trace amounts of wild-type Flag-Mib1 could be co-immunoprecipitated with Myc-Plk4 but, remarkably, strong binding was seen between Plk4 and a Flag-Mib1 Δ RING mutant (Fig. 1C,D), which is catalytically inactive (Berndt et al., 2011; Itoh et al., 2003). Myc-Cep135, analyzed as a control, was unable to bind either wild-type or mutant Mib1 (Fig. 1C). A Mib1 mutant carrying a point mutation (C997S) that disrupts one of the three RING fingers (Berndt et al., 2011) also showed poor binding to Plk4 (Fig. 1C,D), in line with observations that this mutant is at least partially active when overexpressed in cells (Berndt et al., 2011; and data not shown). Using Mib1 deletion mutants (Fig. 1E), binding of Myc-Plk4 could be mapped to the N-terminal but not C-terminal part of Mib1 (Fig. 1C,D). Complex formation could also be detected between Myc-Plk4 and endogenous Mib1 (supplementary material Fig. S2H) and between Plk4 and Mib1 proteins produced by *in vitro* translation (supplementary material Fig. S2I), supporting a direct interaction.

The striking difference in the ability of catalytically active and inactive Mib1 to co-immunoprecipitate with Plk4 raised the possibility that Mib1 might act as an ubiquitin ligase for Plk4. Indeed, transient overexpression of wild-type Flag-Mib1 resulted in the appearance of higher migrating forms of Myc-Plk4 (Fig. 2A), but not Myc-Cep135 (Fig. 2B). Importantly, this Plk4 modification was induced only by Mib1 full length protein, but not by Mib1 deletion mutants (Fig. 2A), even though the latter showed much stronger binding to Plk4 (Fig. 1C,D). To determine the nature of this Mib1-dependent modifications, we co-expressed Myc-Plk4 with His-tagged ubiquitin and either wild-type Flag-Mib1 or Mib1 Δ RING, respectively, and then isolated poly-ubiquitylated protein species. Remarkably, Flag-Mib1 wild-type, but not catalytically inactive Mib1 Δ RING, efficiently promoted poly-ubiquitylation of Myc-Plk4 (Fig. 2C), but not Myc-Cep135 (supplementary material Fig. S3A).

Given that steady-state levels of Plk4 are regulated by the E3 ligase SCF $^{\beta$ -TrCP (Cunha-Ferreira et al., 2009; Guderian et al., 2010; Rogers et al., 2009), we tested the possible involvement of this ligase in Mib1-mediated ubiquitylation of Plk4. As expected,

depletion of β -TrCP caused an increase in active β -catenin (ABC; Fig. 2D), a direct target of SCF $^{\beta$ -TrCP (Hart et al., 1999; van Noort et al., 2002), as well as increased levels of Plk4 at centrosomes (supplementary material Fig. S3B). In striking contrast, β -TrCP depletion did not affect Mib1-induced ubiquitylation of Myc-Plk4 (Fig. 2D), arguing that SCF $^{\beta$ -TrCP does not mediate Mib1 action on Plk4. We have not been able to obtain active full-length Mib1 to demonstrate *in vitro* ubiquitylation of purified Plk4 and thus cannot formally exclude an indirect mechanism. However, the most parsimonious interpretation of our results is that Mib1 acts directly on Plk4.

Next, we used mass spectrometry to explore the nature of the Mib1-induced ubiquitylation of Plk4. We identified a total of 15 ubiquitylated lysine residues within Plk4, many of which clustered within the kinase domain, the linker region, and polo box domains (Fig. 2E). When different moieties of Plk4 were examined for their response to Mib1, most fragments showed a mobility shift after 18 h of co-expression and downregulation after 36 h of co-expression (supplementary material Fig. S3C). In contrast, although mass spectrometry had revealed ubiquitylated lysine residues within the PB1 or PB2 region of Plk4, ubiquitylation of a corresponding fragment (residues 608–970) did not lead to either a mobility upshift or downregulation (supplementary material Fig. S3C). Taken together, these experiments indicate that Mib1 modifies Plk4 on multiple sites, likely involving more than one type of ubiquitylation. Depending on the types of linkages, ubiquitin modifications might either trigger protein degradation or serve to regulate protein localization, activity or protein–protein interactions (Al-Hakim et al., 2008; Ciechanover, 1998; Chen and Sun, 2009; Komander, 2009; Pickart and Eddins, 2004; Xu et al., 2009). To obtain information about the types of Mib1-mediated ubiquitin chains formed on Plk4 we performed ubiquitylation assays using His-ubiquitin mutants that are able to contribute to only one particular type of linkage. Mib1 mediated extensive ubiquitylation of Plk4 in presence of wild-type ubiquitin or mutants conferring K11-, K29- and K48-based linkages, but K63-based ubiquitylation was much less efficient (Fig. 2F). These results suggest that Mib1 is able to induce formation of ubiquitin chains on Plk4 that are typically associated with fast proteasomal degradation (K11 and K48 linkages). In addition, Mib1 clearly induces formation on Plk4 of at least one additional type of ubiquitin chain that is commonly associated with regulatory events (K29 linkages).

Our identification of K11- and K48-based ubiquitin linkages suggested that Mib1 might control Plk4 abundance. To examine this possibility, we transfected Myc-Plk4-inducible U2OS (denoted USOS U2OS:Myc-Plk4) cells with control or Mib1 small interfering RNA (siRNA) oligonucleotides, induced Myc-Plk4 expression by tetracycline and 2 h later added cycloheximide to inhibit protein translation (Fig. 3A). As shown by western blotting (Fig. 3B) and quantified in Fig. 3C, Mib1 depletion led to a significant increase in the levels of exogenous Myc-Plk4. Overexpression of Plk4 in U2OS:Myc-Plk4 cells has been previously shown to trigger centriole over-duplication (Habedanck et al., 2005; Kleylein-Sohn et al., 2007) as reflected in the formation of multiple procentrioles around each pre-existing centriole (Fig. 3D). Interestingly, we found that centriole over-duplication was enhanced upon Mib1 depletion from tetracycline-treated U2OS:Myc-Plk4 cells, particularly when these were synchronized in S phase by aphidicolin, indicating that Mib1 counteracts excess Plk4 activity (Fig. 3E). In contrast, depletion of Mib1 from parental U2OS cells caused neither a significant

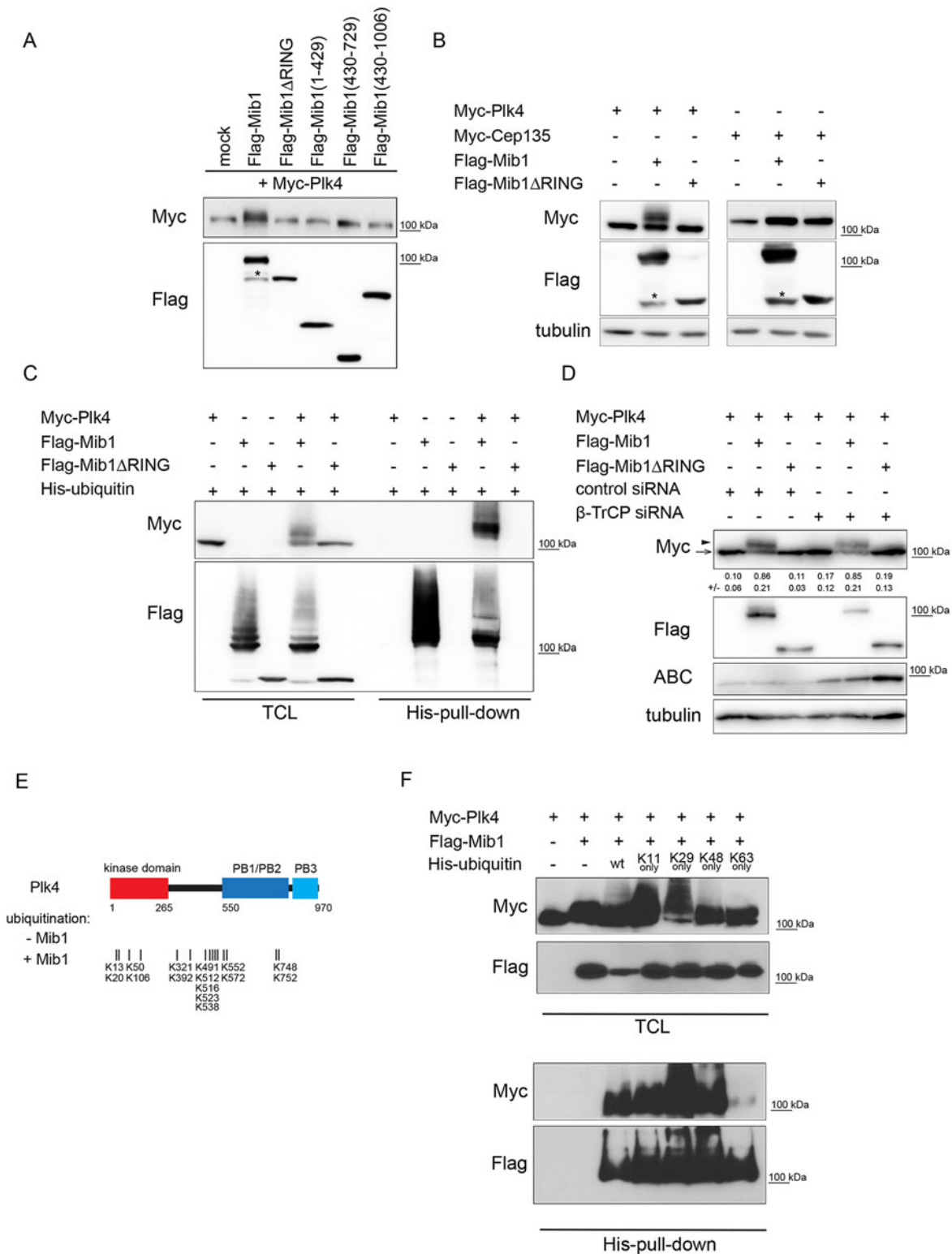


Fig. 2. Mib1 ubiquitylates Plk4. (A,B) HEK293T cells were transfected with Myc–Plk4 (or Myc–Cep135 for control in B) and the indicated Flag–Mib1 constructs before protein extracts were probed by western blotting. The bands marked with an asterisk (*) most likely represent cleavage fragments of Flag–Mib1. (C) HEK293T cells were transfected with the indicated plasmids before His-pull-downs were analyzed by western blotting. (D) HEK293T cells were transfected with the indicated plasmids and subjected to β -TrCP siRNA (or control siRNA) before extracts were probed with antibodies against Myc, Flag, ABC (active β -catenin) and α -tubulin. Numbers below the top panel indicate the signal ratio of modified (arrowhead) to unmodified (arrow) Myc–Plk4, presented as mean \pm s.d. ($n=2$). (E) Schematic representation of ubiquitylated lysine residues (K) within Plk4, as revealed by mass spectrometry (PB, polo box domain). (F) HEK293T cells transfected with the indicated plasmids before His-pull-downs were analyzed by western blotting. His–ubiquitin was used in wild-type form (wt) or in mutant form able to contribute only to specific types of ubiquitin chains, notably, K29-only, K48-only or K63-only. TCL, total cell lysate.

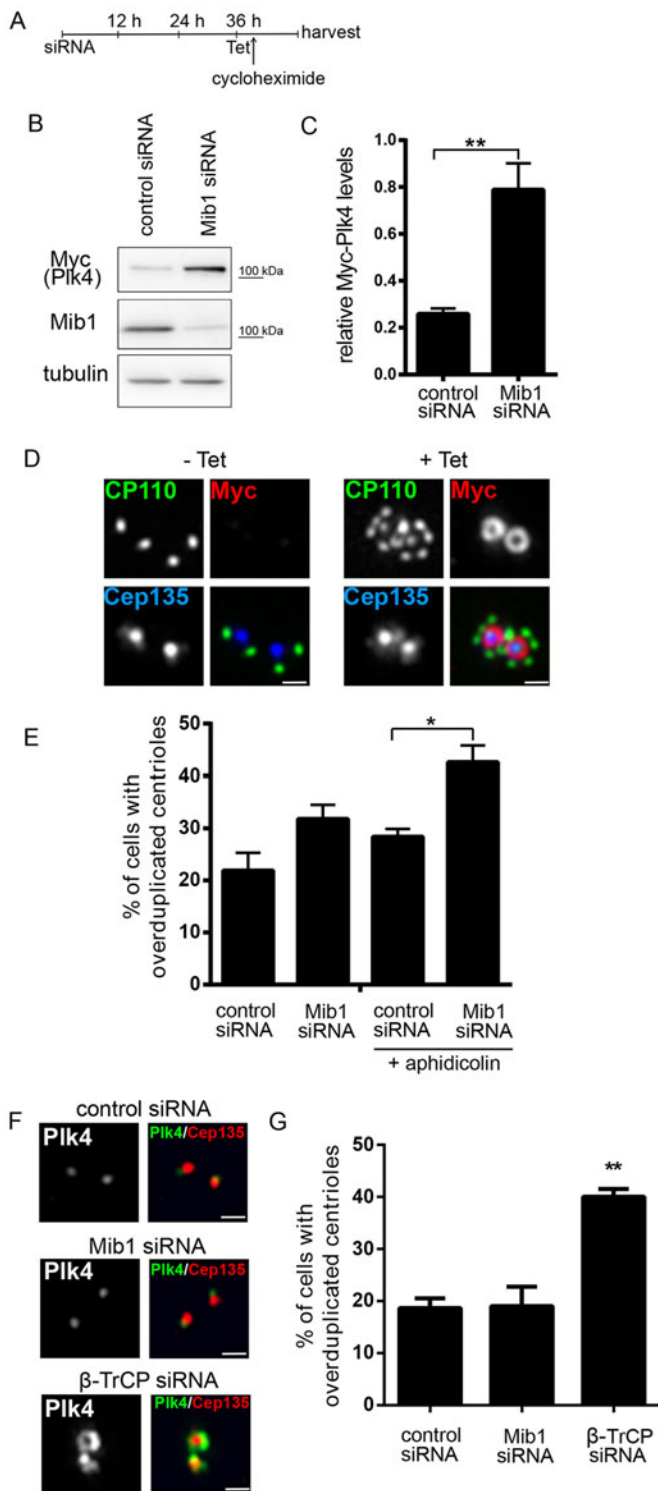


Fig. 3. Mib1 counteracts excessive Plk4 levels. (A) Schematic design of experiments with U2OS:Myc-Plk4 cells, as analyzed in B–E. Tet, tetracycline. (B,C) Western blot analyses of protein extracts prepared from U2OS:Myc-Plk4 cells treated with control or Mib1-specific siRNA. Relative Myc-Plk4 levels (normalized to tubulin, $n=3$, two tailed t -test, $**P=0.0045$) are quantified in C. (D) Non-induced (–Tet) and induced (+Tet) U2OS:Myc-Plk4 cells were fixed and stained for CP110 (green), Myc-Plk4 (red), and the centriole maker Cep135 (blue). Scale bar: 0.5 μm . (E) Quantification of Myc-Plk4-induced centriole over-duplication (more than four CP110-positive centrioles per cell) in asynchronously growing or S-phase arrested (aphidicolin-treated) U2OS cells subjected to control or Mib1-specific siRNA (mean \pm s.e.m., $n=4$, one way-ANOVA). $*P<0.05$. (F) U2OS cells were treated with the indicated siRNA oligonucleotides and stained after 48 h for Plk4 (green) and Cep135 (red). Scale bar: 0.5 μm . (G) Quantification (mean \pm s.e.m., $n=3$, one way-ANOVA) of the effects of the indicated siRNA treatments on centriole over-duplication (counted as in E). $**P<0.01$.

centrioles (Fig. 4A,B), and similar effects were seen also upon endogenous Plk4 (Fig. 4C,D). Similarly, Mib1 caused downregulation when Plk4 levels were elevated by β -TrCP depletion (supplementary material Fig. S4A,B), and expression of Flag-Mib1 in the U2OS:Myc-Plk4 cell line greatly impaired the ability of exogenous Myc-Plk4 to trigger centriole over-duplication (Fig. 4E,F). Taken together, these results demonstrate that Mib1 is able to reduce centriolar levels of Plk4 and thereby counteract Plk4-induced centriole over-duplication. Flag-Mib1 overexpression also caused a reduction in centriolar levels of Sas6 (supplementary material Fig. S4C,D), in line with recent studies showing that Plk4 is required for the recruitment of Sas6 to centrioles (Dzhindzhev et al., 2014; Kratz et al., 2015; Ohta et al., 2014). Interestingly, Mib1 also caused a mobility upshift in Sas6, but not in STIL (supplementary material Fig. S4E). The significance of this upshift will require further study. One possibility is that Sas6 is an additional target of Mib1, in which case Sas6 ubiquitylation might also contribute to the effects of Mib1 on centriole duplication.

In addition to K48-linked ubiquitin chains, we observed ubiquitin chains on Plk4 that are not generally related to fast proteasomal protein degradation (Al-Hakim et al., 2008; Komander, 2009; Xu et al., 2009). This most likely explains why Mib1-induced ubiquitylated species of Plk4 could readily be detected without use of proteasome inhibitors (Fig. 3A–C). Considering that we were able to map ubiquitylated lysine residues to regions that are essential for Plk4 functionality, notably the kinase domain, the linker region and the polo box domains (Fig. 2E), we asked whether ubiquitylation might affect the interaction of Plk4 with its binding partners Cep192 and Cep152 (Cizmecioglu et al., 2010; Dzhindzhev et al., 2010; Hatch et al., 2010; Kim et al., 2013; Sonnen et al., 2013). We found that affinity purified LAP-Plk4, ubiquitylated in a Mib1-dependent manner, indeed showed reduced *in vitro* binding to both the GST-tagged N-terminal of Cep192 and Cep152 (Fig. 4G–I). Taken together, these results suggest that ubiquitylation by Mib1 negatively affects the ability of Plk4 to bind its centriole-recruitment factors Cep152 and Cep192 (Kim et al., 2013; Sonnen et al., 2013).

In conclusion, we show that Mib1 is important for regulating Plk4 levels, particularly under conditions of aberrant Plk4 expression. Such conditions are known to occur in breast cancer as well as other tumor types (Chng et al., 2008; Macmillan et al., 2001; Mason et al., 2014; van de Vijver et al., 2002). Specifically, we propose that SCF $^{\beta\text{-TrCP}}$ is the major E3 ligase controlling steady-state Plk4 levels under physiological conditions (Cunha-Ferreira et al., 2013; Cunha-Ferreira et al.,

increase in centrosomal levels of Plk4 (Fig. 3F) nor centriole amplification (Fig. 3G), although both these phenotypes could readily be observed upon depletion of β -TrCP (Fig. 3F,G). These results suggest that the ubiquitin ligase activity of Mib1 becomes important primarily in response to excess Plk4, whereas normal cell cycle regulation is exerted primarily by SCF $^{\beta\text{-TrCP}}$.

We also examined the impact of Mib1 overexpression on Plk4 levels. We found that overexpression of Flag-Mib1, but not Flag-Mib1 Δ RING, caused a marked decrease of Myc-Plk4 levels at

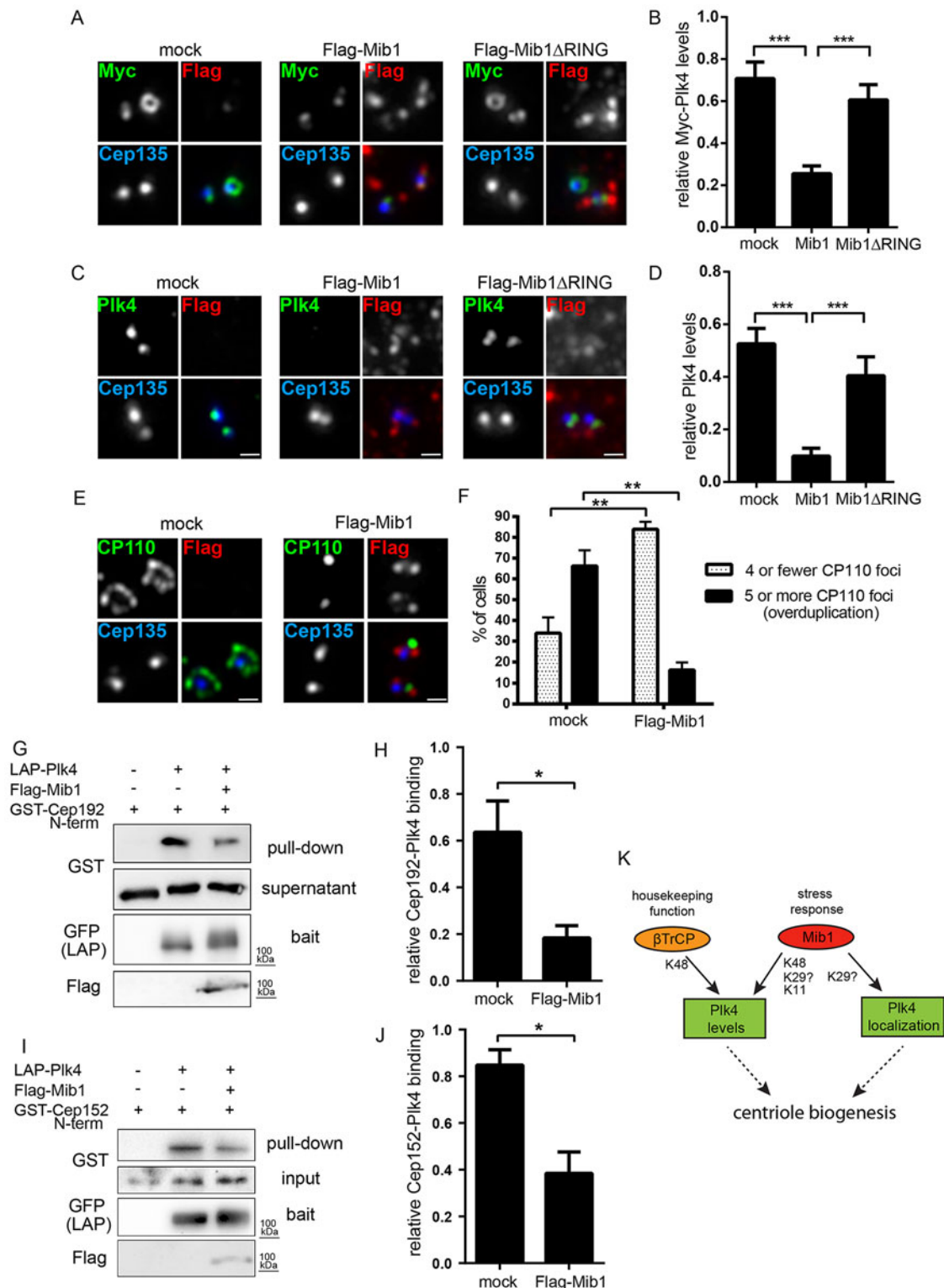


Fig. 4. Mib1 negatively regulates centriole biogenesis and Plk4 interactions. (A,B) U2OS:Myc-Pik4 cells were transfected with the indicated plasmids, treated for 2 h with tetracycline and then stained for Myc-Pik4 (green), Flag-Mib1 (red) and the centriole marker Cep135 (blue). A quantification (mean±s.e.m., $n=3$, one way-ANOVA) is shown in B. (C) U2OS cells were transfected with the indicated plasmids and stained for endogenous Plk4 (green), Flag-Mib1 (red) and Cep135 (blue). Quantification (mean±s.e.m., $n=2$, one way-ANOVA) is shown in D. (E) Transfected U2OS:Myc-Pik4 cells were treated for 6 h with tetracycline and stained for CP110 (green), Flag-Mib1 (red) and Cep135 (blue). Quantification (mean±s.e.m., $n=3$, two way-ANOVA) is shown in F. (G,I) Western blot analyses of the effect of Mib1-mediated ubiquitylation on binding of affinity-purified LAP-Pik4 to the GST-tagged Cep192 N-terminus (G) or GST-tagged Cep152 N-terminus (I). Quantification of these results is shown in H (mean±s.e.m., $n=4$, two tailed t -test, $*P=0.0315$) and J (mean±s.e.m., $n=3$, two tailed t -test, $*P=0.0148$), respectively. (K) Proposed model, as described in text. Scale bars: 0.5 μ m.

2009; Holland et al., 2012; Klebba et al., 2013) and that Mib1 might become important primarily in response to excess Plk4 (this study). As illustrated in Fig. 4K, our data indicate that Mib1-induced ubiquitylation results in at least two functional consequences for Plk4 and hence centriole numbers. First, Mib1 contributes to control turnover of Plk4 through ubiquitin-dependent proteolytic degradation. Second, Mib1-dependent ubiquitylation of Plk4 also impairs the ability of Plk4 to interact with Cep152 and Cep192, hence reducing its association with centrioles. Combined, these Mib1-induced effects on Plk4 abundance and localization contribute to control centriole numbers. In future it will be interesting to explore the role of Mib1 in the control of Plk4 under pathophysiological conditions, notably in human tumors with high levels of centriole amplification. As one example, we have shown here that Mib1 levels are enhanced at the centrioles of breast cancer cells, MCF-7, which express higher levels of Plk4 than RPE-1 cells, and our model would indicate that this reflects a response to deregulation of Plk4. However, it is also attractive to speculate that tumors might exist in which a loss of Mib1 (or Mib2) activity causes Plk4 overexpression and concomitant centriole duplication.

MATERIALS AND METHODS

Cell culture, transfections and drug treatments

U2OS, U2OS:Myc-Plk4 (Kleylein-Sohn et al., 2007), MCF-7 and HEK293T cells were propagated in Dulbecco's modified Eagle's medium (DMEM), and RPE-1 cells were grown in DMEM with F12. Media were supplemented with 10% fetal bovine serum (FBS) and penicillin-streptomycin (all from Life Technologies, Carlsbad, CA; FBS for U2OS:Myc-Plk4 from PAA). Transfection was performed with TransIT-LT1 (Mirus Bio, Madison, WI). siRNA experiments were performed using Oligofectamine (U2OS cell) or Lipofectamine RNAiMAX (HEK293T cells), both from Life Technologies. Control (GL2) and Mib1 (targeting sequence, TTCTCATCCACAATCCA-TGGT), PCM-1 (targeting sequence, AATCAGCTTCGTGATTCT-CAG), or β -TrCP1 and β -TrCP2 (targeting sequence, GTGGAATTTGT-GGAACATC) specific oligonucleotides were used at concentrations of 50–100 nM for 36–48 h. In some experiments, cells were transfected with plasmids 32–36 h after siRNA transfection, as described above. Expression of Myc-Plk4 in the U2OS:Myc-Plk4 cell line was induced by tetracycline (1 μ g/ml) for 2–12 h. Where indicated, cells were treated with cycloheximide (50 μ g/ml) or aphidicolin (1.6 μ g/ml; 24 h).

Plasmids and cloning

Insert-containing entry vectors for use in the GATEWAY system (Life Technologies) were generated by PCR, using Pfu Ultra II Fusion DNA polymerase (Agilent, Santa Clara, CA). Inserts were verified by sequencing and subsequently cloned into pDEST-Myc, pDEST-Flag, pDEST-GST (Invitrogen), or pg-LAP1 (Addgene plasmid 19702) GATEWAY destination vectors. All human cDNAs used here have been described previously: Mib1 (Berndt et al., 2011), Plk4 (Habedanck et al., 2005), Cep152 and Cep192 (Sonnen et al., 2013), Cep135 (Kleylein-Sohn et al., 2007), Ubiquitin wt and chain-specific mutants (Chastagner et al., 2006).

Immunofluorescence microscopy

Methanol fixation of cells, blocking, incubation with primary and secondary antibodies, and washing were performed as described (Sonnen et al., 2012). The following antibodies were used: rabbit anti-PCM-1 was raised by Charles River Laboratories against His-PCM-1 (amino acids 1022–1202), rabbit anti-Mib1 (M5948; Sigma-Aldrich, St. Louis, MI), rabbit anti-Cep135, rabbit-CP110, rabbit anti-Plk4 (all described in Kleylein-Sohn et al., 2007), mouse anti-Plk4 (Guderian et al., 2010), mouse anti-Myc (clone 9E10), mouse anti-Flag (clone M2; Sigma-Aldrich), Alexa-Fluor-488-conjugated donkey anti-mouse, Alexa-Fluor-488-conjugated donkey anti-rabbit, Alexa-Fluor-488-conjugated donkey anti-mouse, and Alexa-Fluor-488-conjugated donkey anti-rabbit (all from

Life Technologies). Direct labeling of primary antibodies was performed using an Alexa-antibody labeling kit (Life Technologies). Imaging was performed in Glycergel mounting medium (Agilent) at room temperature, using a DeltaVision Core system (Applied Precision, Issaquah, WA) with a 60 \times /1.2 or 100 \times /1.4 Apo plan oil immersion objective, Photometrics CoolSNAP CCD camera and solid state illumination. Image stacks were taken with a z distance of 0.2 μ m, deconvolved (conservative ratio, three to five cycles), and projected as maximal intensity images by using SoftWoRX (Applied Precision). For cell counts, 50–100 cells per condition and experiment were analyzed. Densitometry analysis was performed in 16-bit TIFF images with ImageJ within selected regions of interest (ROIs); 15–20 cells per experiment and condition were analyzed. Data are presented as relative staining intensity (staining intensity of a protein of interest normalized to the intensity of centriolar marker Cep135). Relative Mib1 levels at the centrosome (supplementary material Fig. S2G) were measured as total intensities in ROIs using Cell Profiler. The area of Cep135 signal, enlarged by 2ppx, was used to create a mask to measure centriole-associated Mib1 staining. Contrast and/or brightness adjustment and cropping of final images were done using Photoshop CS5 (Adobe Systems, San Jose, CA).

Cell lysis, pulldown and western blotting

At 18 h post-transfection, cells were washed in PBS and lysed [62.5 mM Tris-HCl, pH 6.8, 1% SDS, 10% glycerol (all from Sigma-Aldrich)]. Samples were processed as described previously (Bryja et al., 2005) and analyzed by western blotting. The following antibodies were used, in addition to those listed above: rabbit anti-Myc (sc-789; Santa Cruz Biotechnology, Dallas, TX), rabbit anti-Flag (F7425; Sigma-Aldrich), goat anti-GST (27457701V; GE Healthcare, Issaquah, WA), rabbit anti-GFP (Ab290; Roche, Basel, Switzerland), mouse anti- α -tubulin (T9026; Sigma-Aldrich), mouse anti-active- β -catenin (clone 8E7; Millipore, Billerica, MA), horseradish peroxidase (HRP)-conjugated goat anti-mouse (170-6516) and goat anti-rabbit (170-6515, both from BioRad, Hercules, CA), and HRP-conjugated donkey anti-goat (sc-2020; Santa Cruz Biotechnology). Signal was revealed using the SuperSignal Femto detection kit (Thermo Scientific, Rockford, IL) and detected using LAS3000 (GE Healthcare), ChemiDoc (BioRad) or film (Fig. 2F, Agfa). For immunoprecipitation–pulldown experiments, cells were lysed in IP Lysis buffer [20 mM Tris-HCl pH 7.4, 150 mM NaCl, 25 mM β -glycerol phosphate, 0.5% Igepal CA630, 0.5% Triton X-100 (all from Sigma-Aldrich), and 1 \times Complete proteasome inhibitors (Roche)]. Following centrifugation (15,000 g for 10 min at +4 $^{\circ}$ C), cleared extracts were incubated (6 h at +4 $^{\circ}$ C in an orbital shaker) with anti-Myc (9E10), anti-Flag (M2) G-protein–sepharose (GE Healthcare) or S-protein agarose (Novagen, Billerica, MA). Each batch of beads with LAP–Plk4 was tested for the presence of a Mib1-induced upshift and stored as a 25% slurry (IP Lysis buffer plus 10% glycerol and 100 μ M DTT; –80 $^{\circ}$ C) until used in binding assays. His pulldowns were performed in denaturing conditions [50 mM Tris-HCl, pH 7.4, 300 mM NaCl, 0.5% Triton-X-100, 0.05% SDS, 10 mM Imidazol and 6 M Urea (all from Sigma-Aldrich)] using Ni-NTA agarose (Qiagen, Hilden, Germany). Complexes were pelleted, washed, and subsequently analyzed by western blotting.

In vitro translation, recombinant protein purification and binding assays

Myc-Plk4, Flag–Mib1 and Flag–Cep152 were translated *in vitro* (TNT Quick system; Promega, Madison, WI), mixed with modified IP Lysis buffer (as above; 0.05% Igepal CA630, 100 μ M DTT) and subjected to immunoprecipitation and washing. GST-tagged proteins were purified as described previously (Čajánek and Nigg, 2014). Binding of Mib1-modified LAP–Plk4 with the GST-tagged Cep192 N-terminus (recombinant, purified from bacteria) or Cep152 N-terminus (translated *in vitro*) was performed in pulldown buffer (20 mM Tris-HCl, pH 7.4, 150 mM NaCl, 25 mM β -glycerol phosphate, 0.5% Igepal CA630, 100 μ M DTT) for 45 min (+4 $^{\circ}$ C; orbital shaker). Where indicated, densitometry analysis of blots was performed with ImageJ or ImageLab (Fig. 2D; BioRad).

Mass spectrometry analyses of ubiquitination

Following 4 h of treatment with proteasome inhibitor MG132 (10 μ M), LAP–Plk4 was isolated from HEK293T cell extracts prepared 18 h after transfection, using S-protein agarose. Proteins were eluted, reduced, alkylated, digested with trypsin overnight, and then purified with C-18 Microspin columns (Harvard Apparatus, Holliston, MA). Peptides were separated by using an Easy-Nano-LC system, and liquid-chromatography–tandem-MS analysis was performed on a hybrid LTQ-Orbitrap mass spectrometer (both from Thermo Scientific). Obtained protein spectra were searched against the human proteome database (UniProt). The detection of ligated ubiquitin was based on ubiquitin-derived di-glycine mass increments of ubiquitylated peptides (114.1 Da per modified lysine residue) (Kirkpatrick et al., 2005).

Statistical analyses

Statistical analyses (Student's *t*-test or ANOVA with Tukey's multiple comparison test) were performed using Prism 6 (GraphPad Software, La Jolla, CA). **P*<0.05, ***P*<0.01 and ****P*<0.001 were considered statistically significant differences. Results are presented as mean \pm s.e.m.

Acknowledgements

We thank Jason Berndt (University of Washington), Christel Brou (Institut Pasteur), Peter Jackson (Genentech), Matthias Peter (ETH Zurich), Xiumin Yan (IBCB Shanghai), Christian Arqunt, and Patrick Redli (both Biozentrum) for sharing reagents, Gernot Guderian for communicating initial observations on a possible Mib1–Plk4 interaction, and Elena Nigg, the imaging core facility and the proteomics core facility for assistance.

Competing interests

The authors declare no competing or financial interests.

Author contributions

L.C. was responsible for conception and design, collection and/or assembly of data, data analyses and interpretation and manuscript writing; T.G. responsible for collection and/or assembly of data; E.A.N. was responsible for conception and design, data interpretation, manuscript writing.

Funding

This work was supported by the Swiss National Science Foundation [grant number 310030B_149641]; and the University of Basel. L.C. acknowledges support from the Federation of European Biochemical Societies (long-term fellowship), and Masaryk University, Faculty of Medicine [grant number MUNI/11/InGA15/2014].

Supplementary material

Supplementary material available online at <http://jcs.biologists.org/lookup/suppl/doi:10.1242/jcs.166496/-DC1>

References

- Akimov, V., Rigbolt, K. T., Nielsen, M. M. and Blagoev, B. (2011). Characterization of ubiquitination dependent dynamics in growth factor receptor signaling by quantitative proteomics. *Mol. Biosyst.* **7**, 3223–3233.
- Al-Hakim, A. K., Zagorska, A., Chapman, L., Deak, M., Pegg, M. and Alessi, D. R. (2008). Control of AMPK-related kinases by USP9X and atypical Lys(29)/Lys(33)-linked polyubiquitin chains. *Biochem. J.* **411**, 249–260.
- Azimzadeh, J. and Bornens, M. (2007). Structure and duplication of the centrosome. *J. Cell Sci.* **120**, 2139–2142.
- Balczon, R., Bao, L. and Zimmer, W. E. (1994). PCM-1, A 228-kD centrosome autoantigen with a distinct cell cycle distribution. *J. Cell Biol.* **124**, 783–793.
- Barsi, J. C., Rajendra, R., Wu, J. I. and Artzt, K. (2005). Mind bomb1 is a ubiquitin ligase essential for mouse embryonic development and Notch signaling. *Mech. Dev.* **122**, 1106–1117.
- Berndt, J. D., Aoyagi, A., Yang, P., Anastas, J. N., Tang, L. and Moon, R. T. (2011). Mindbomb 1, an E3 ubiquitin ligase, forms a complex with RYK to activate Wnt/ β -catenin signaling. *J. Cell Biol.* **194**, 737–750.
- Bettencourt-Dias, M., Rodrigues-Martins, A., Carpenter, L., Riparbelli, M., Lehmann, L., Gatt, M. K., Carmo, N., Balloux, F., Callaini, G. and Glover, D. M. (2005). SAK/PLK4 is required for centriole duplication and flagella development. *Curr. Biol.* **15**, 2199–2207.
- Bettencourt-Dias, M., Hildebrandt, F., Pellman, D., Woods, G. and Godinho, S. A. (2011). Centrosomes and cilia in human disease. *Trends Genet.* **27**, 307–315.
- Bornens, M. (2012). The centrosome in cells and organisms. *Science* **335**, 422–426.
- Bryja, V., Čajánek, L., Pacherník, J., Hall, A. C., Horváth, V., Dvůrák, P. and Hampl, A. (2005). Abnormal development of mouse embryoid bodies lacking p27Kip1 cell cycle regulator. *Stem Cells* **23**, 965–974.
- Čajánek, L. and Nigg, E. A. (2014). Cep164 triggers ciliogenesis by recruiting Tau tubulin kinase 2 to the mother centriole. *Proc. Natl. Acad. Sci. USA* **111**, E2841–E2850.
- Chastagner, P., Israël, A. and Brou, C. (2006). Itch/AIP4 mediates Deltex degradation through the formation of K29-linked polyubiquitin chains. *EMBO Rep.* **7**, 1147–1153.
- Chavali, P. L., Pütz, M. and Gergely, F. (2014). Small organelle, big responsibility: the role of centrosomes in development and disease. *Philos. Trans. R. Soc. B* **369**, 369.
- Chen, Z. J. and Sun, L. J. (2009). Nonproteolytic functions of ubiquitin in cell signaling. *Mol. Cell* **33**, 275–286.
- Chng, W. J., Braggio, E., Mulligan, G., Bryant, B., Remstein, E., Valdez, R., Dogan, A. and Fonseca, R. (2008). The centrosome index is a powerful prognostic marker in myeloma and identifies a cohort of patients that might benefit from aurora kinase inhibition. *Blood* **111**, 1603–1609.
- Ciechanover, A. (1998). The ubiquitin-proteasome pathway: on protein death and cell life. *EMBO J.* **17**, 7151–7160.
- Cizmecioglu, O., Arnold, M., Bahtz, R., Settele, F., Ehret, L., Haselmann-Weiss, U., Antony, C. and Hoffmann, I. (2010). Cep152 acts as a scaffold for recruitment of Plk4 and CPAP to the centrosome. *J. Cell Biol.* **191**, 731–739.
- Cunha-Ferreira, I., Rodrigues-Martins, A., Bento, I., Riparbelli, M., Zhang, W., Laue, E., Callaini, G., Glover, D. M. and Bettencourt-Dias, M. (2009). The SCF/Slimb ubiquitin ligase limits centrosome amplification through degradation of SAK/PLK4. *Curr. Biol.* **19**, 43–49.
- Cunha-Ferreira, I., Bento, I., Pimenta-Marques, A., Jana, S. C., Lince-Faria, M., Duarte, P., Borrego-Pinto, J., Gilberto, S., Amado, T., Brito, D. et al. (2013). Regulation of autophosphorylation controls PLK4 self-destruction and centrosome number. *Curr. Biol.* **23**, 2245–2254.
- D'Assoro, A. B., Busby, R., Suino, K., Delva, E., Almodovar-Mercado, G. J., Johnson, H., Folk, C., Farrugia, D. J., Vasile, V., Stivala, F. et al. (2004). Genotoxic stress leads to centrosome amplification in breast cancer cell lines that have an inactive G1/S cell cycle checkpoint. *Oncogene* **23**, 4068–4075.
- Dammermann, A. and Merdes, A. (2002). Assembly of centrosomal proteins and microtubule organization depends on PCM-1. *J. Cell Biol.* **159**, 255–266.
- Daskalaki, A., Shalaby, N. A., Kux, K., Tsoumpikos, G., Tsiibidis, G. D., Muskavitch, M. A. and Delidakis, C. (2011). Distinct intracellular motifs of Delta mediate its ubiquitylation and activation by Mindbomb1 and Neuralized. *J. Cell Biol.* **195**, 1017–1031.
- Dzhindzhev, N. S., Yu, Q. D., Weiskopf, K., Tzolovsky, G., Cunha-Ferreira, I., Riparbelli, M., Rodrigues-Martins, A., Bettencourt-Dias, M., Callaini, G. and Glover, D. M. (2010). Asterless is a scaffold for the onset of centriole assembly. *Nature* **467**, 714–718.
- Dzhindzhev, N. S., Tzolovsky, G., Lipinski, Z., Schneider, S., Lattao, R., Fu, J., Debski, J., Dadez, M. and Glover, D. M. (2014). Plk4 phosphorylates Ana2 to trigger Sas6 recruitment and procentriole formation. *Curr. Biol.* **24**, 2526–2532.
- Firat-Karalar, E. N. and Stearns, T. (2014). The centriole duplication cycle. *Philos. Trans. R. Soc. B* **369**, 369.
- Godinho, S. A. and Pellman, D. (2014). Causes and consequences of centrosome abnormalities in cancer. *Philos. Trans. R. Soc. B* **369**, 20130467.
- Gönczy, P. (2012). Towards a molecular architecture of centriole assembly. *Nat. Rev. Mol. Cell Biol.* **13**, 425–435.
- Guderian, G., Westendorf, J., Uldschmid, A. and Nigg, E. A. (2010). Plk4 trans-autophosphorylation regulates centriole number by controlling betaTrCP-mediated degradation. *J. Cell Sci.* **123**, 2163–2169.
- Habedanck, R., Stierhof, Y. D., Wilkinson, C. J. and Nigg, E. A. (2005). The Polo kinase Plk4 functions in centriole duplication. *Nat. Cell Biol.* **7**, 1140–1146.
- Hart, M., Concordet, J. P., Lassot, I., Albert, I., del los Santos, R., Durand, H., Perret, C., Rubinfeld, B., Margottin, F., Benarous, R. et al. (1999). The F-box protein beta-TrCP associates with phosphorylated beta-catenin and regulates its activity in the cell. *Curr. Biol.* **9**, 207–211.
- Hatch, E. M., Kulukian, A., Holland, A. J., Cleveland, D. W. and Stearns, T. (2010). Cep152 interacts with Plk4 and is required for centriole duplication. *J. Cell Biol.* **191**, 721–729.
- Hildebrandt, F., Benzing, T. and Katsanis, N. (2011). Ciliopathies. *N. Engl. J. Med.* **364**, 1533–1543.
- Holland, A. J., Lan, W., Niessen, S., Hoover, H. and Cleveland, D. W. (2010). Polo-like kinase 4 kinase activity limits centrosome overduplication by autoregulating its own stability. *J. Cell Biol.* **188**, 191–198.
- Holland, A. J., Fachinetti, D., Zhu, Q., Bauer, M., Verma, I. M., Nigg, E. A. and Cleveland, D. W. (2012). The autoregulated instability of Polo-like kinase 4 limits centrosome duplication to once per cell cycle. *Genes Dev.* **26**, 2684–2689.
- Ishikawa, H. and Marshall, W. F. (2011). Ciliogenesis: building the cell's antenna. *Nat. Rev. Mol. Cell Biol.* **12**, 222–234.
- Itoh, M., Kim, C. H., Palardy, G., Oda, T., Jiang, Y. J., Maust, D., Yeo, S. Y., Lorick, K., Wright, G. J., Ariza-McNaughton, L. et al. (2003). Mind bomb is a ubiquitin ligase that is essential for efficient activation of Notch signaling by Delta. *Dev. Cell* **4**, 67–82.
- Jakobsen, L., Vanselow, K., Skogs, M., Toyoda, Y., Lundberg, E., Poser, I., Falkenby, L. G., Bennetzen, M., Westendorf, J., Nigg, E. A. et al. (2011). Novel asymmetrically localizing components of human centrosomes identified by complementary proteomics methods. *EMBO J.* **30**, 1520–1535.
- Kim, T. S., Park, J. E., Shukla, A., Choi, S., Murugan, R. N., Lee, J. H., Ahn, M., Rhee, K., Bang, J. K., Kim, B. Y. et al. (2013). Hierarchical recruitment of Plk4

- and regulation of centriole biogenesis by two centrosomal scaffolds, Cep192 and Cep152. *Proc. Natl. Acad. Sci. USA* **110**, E4849–E4857.
- Kirkpatrick, D. S., Denison, C. and Gygi, S. P.** (2005). Weighing in on ubiquitin: the expanding role of mass-spectrometry-based proteomics. *Nat. Cell Biol.* **7**, 750–757.
- Klebba, J. E., Buster, D. W., Nguyen, A. L., Swatkoski, S., Gucek, M., Rusan, N. M. and Rogers, G. C.** (2013). Polo-like kinase 4 autodeconstructs by generating its Slimb-binding phosphodegron. *Curr. Biol.* **23**, 2255–2261.
- Kleylein-Sohn, J., Westendorf, J., Le Clech, M., Habedanck, R., Stierhof, Y. D. and Nigg, E. A.** (2007). Plk4-induced centriole biogenesis in human cells. *Dev. Cell* **13**, 190–202.
- Komander, D.** (2009). The emerging complexity of protein ubiquitination. *Biochem. Soc. Trans.* **37**, 937–953.
- Kratz, A. S., Barenz, F., Richter, K. T. and Hoffmann, I.** (2015). Plk4-dependent phosphorylation of STIL is required for centriole duplication. *Biol. Open* **4**, 370–377.
- Li, S., Wang, L., Berman, M., Kong, Y. Y. and Dorf, M. E.** (2011). Mapping a dynamic innate immunity protein interaction network regulating type I interferon production. *Immunity* **35**, 426–440.
- Liu, L. J., Liu, T. T., Ran, Y., Li, Y., Zhang, X. D., Shu, H. B. and Wang, Y. Y.** (2012). The E3 ubiquitin ligase MIB1 negatively regulates basal I κ B α level and modulates NF- κ B activation. *Cell Res.* **22**, 603–606.
- Lopes, C. A., Prosser, S. L., Romio, L., Hirst, R. A., O'Callaghan, C., Woolf, A. S. and Fry, A. M.** (2011). Centriolar satellites are assembly points for proteins implicated in human ciliopathies, including oral-facial-digital syndrome 1. *J. Cell Sci.* **124**, 600–612.
- Macmillan, J. C., Hudson, J. W., Bull, S., Dennis, J. W. and Swallow, C. J.** (2001). Comparative expression of the mitotic regulators SAK and PLK in colorectal cancer. *Ann. Surg. Oncol.* **8**, 729–740.
- Martin, C. A., Ahmad, I., Klingseisen, A., Hussain, M. S., Bicknell, L. S., Leitch, A., Nurnberg, G., Toliat, M. R., Murray, J. E., Hunt, D. et al.** (2014). Mutations in PLK4, encoding a master regulator of centriole biogenesis, cause microcephaly, growth failure and retinopathy. *Nat. Genet.* **46**, 1283–1292.
- Mason, J. M., Lin, D. C., Wei, X., Che, Y., Yao, Y., Kiarash, R., Cescon, D. W., Fletcher, G. C., Awrey, D. E., Bray, M. R. et al.** (2014). Functional characterization of CFI-400945, a Polo-like kinase 4 inhibitor, as a potential anticancer agent. *Cancer Cell* **26**, 163–176.
- Nigg, E. A. and Raff, J. W.** (2009). Centrioles, centrosomes, and cilia in health and disease. *Cell* **139**, 663–678.
- Nigg, E. A. and Stearns, T.** (2011). The centrosome cycle: Centriole biogenesis, duplication and inherent asymmetries. *Nat. Cell Biol.* **13**, 1154–1160.
- Nigg, E. A., Cajánek, L. and Arquint, C.** (2014). The centrosome duplication cycle in health and disease. *FEBS Lett.* **588**, 2366–2372.
- O'Connell, K. F., Caron, C., Kopish, K. R., Hurd, D. D., Kempfues, K. J., Li, Y. and White, J. G.** (2001). The *C. elegans* zyg-1 gene encodes a regulator of centrosome duplication with distinct maternal and paternal roles in the embryo. *Cell* **105**, 547–558.
- Ohta, M., Ashikawa, T., Nozaki, Y., Kozuka-Hata, H., Goto, H., Inagaki, M., Oyama, M. and Kitagawa, D.** (2014). Direct interaction of Plk4 with STIL ensures formation of a single procentriole per parental centriole. *Nat. Commun.* **5**, 5267.
- Pickart, C. M. and Eddins, M. J.** (2004). Ubiquitin: structures, functions, mechanisms. *Biochim. Biophys. Acta* **1695**, 55–72.
- Rodrigues-Martins, A., Riparbelli, M., Callaini, G., Glover, D. M. and Bettencourt-Dias, M.** (2007). Revisiting the role of the mother centriole in centriole biogenesis. *Science* **316**, 1046–1050.
- Rogers, G. C., Rusan, N. M., Roberts, D. M., Peifer, M. and Rogers, S. L.** (2009). The SCF Slimb ubiquitin ligase regulates Plk4/Sak levels to block centriole reduplication. *J. Cell Biol.* **184**, 225–239.
- Santos, N. and Reiter, J. F.** (2008). Building it up and taking it down: the regulation of vertebrate ciliogenesis. *Dev. Dyn.* **237**, 1972–1981.
- Sillibourne, J. E., Tack, F., Vloemans, N., Boeckx, A., Thambirajah, S., Bonnet, P., Ramaekers, F. C., Bornens, M. and Grand-Perret, T.** (2010). Autophosphorylation of polo-like kinase 4 and its role in centriole duplication. *Mol. Biol. Cell* **21**, 547–561.
- Sonnen, K. F., Schermelleh, L., Leonhardt, H. and Nigg, E. A.** (2012). 3D-structured illumination microscopy provides novel insight into architecture of human centrosomes. *Biol. Open* **1**, 965–976.
- Sonnen, K. F., Gabryjonczyk, A. M., Anselm, E., Stierhof, Y. D. and Nigg, E. A.** (2013). Human Cep192 and Cep152 cooperate in Plk4 recruitment and centriole duplication. *J. Cell Sci.* **126**, 3223–3233.
- Stowe, T. R., Wilkinson, C. J., Iqbal, A. and Stearns, T.** (2012). The centriolar satellite proteins Cep72 and Cep290 interact and are required for recruitment of BBS proteins to the cilium. *Mol. Biol. Cell* **23**, 3322–3335.
- Thornton, G. K. and Woods, C. G.** (2009). Primary microcephaly: do all roads lead to Rome? *Trends Genet.* **25**, 501–510.
- Tollenaere, M. A., Mailand, N. and Bekker-Jensen, S.** (2014). Centriolar satellites: key mediators of centrosome functions. *Cell. Mol. Life Sci.* **72**, 11–23.
- Tseng, L. C., Zhang, C., Cheng, C. M., Xu, H., Hsu, C. H. and Jiang, Y. J.** (2014). New classes of mind bomb-interacting proteins identified from yeast two-hybrid screens. *PLoS ONE* **9**, e93394.
- van de Vijver, M. J., He, Y. D., van't Veer, L. J., Dai, H., Hart, A. A., Voskuil, D. W., Schreiber, G. J., Peterse, J. L., Roberts, C., Marton, M. J. et al.** (2002). A gene-expression signature as a predictor of survival in breast cancer. *N. Engl. J. Med.* **347**, 1999–2009.
- van Noort, M., Meeldijk, J., van der Zee, R., Destree, O. and Clevers, H.** (2002). Wnt signaling controls the phosphorylation status of beta-catenin. *J. Biol. Chem.* **277**, 17901–17905.
- Villumsen, B. H., Danielsen, J. R., Povlsen, L., Sylvestersen, K. B., Merdes, A., Beli, P., Yang, Y. G., Choudhary, C., Nielsen, M. L., Mailand, N. et al.** (2013). A new cellular stress response that triggers centriolar satellite reorganization and ciliogenesis. *EMBO J.* **32**, 3029–3040.
- Xu, P., Duong, D. M., Seyfried, N. T., Cheng, D., Xie, Y., Robert, J., Rush, J., Hochstrasser, M., Finley, D. and Peng, J.** (2009). Quantitative proteomics reveals the function of unconventional ubiquitin chains in proteasomal degradation. *Cell* **137**, 133–145.